Extended Abstracts of the 2009 International Conference on Solid State Devices and Materials, Sendai, 2009, pp350-351

Improvement of Cu seedless Ru barrier by insertion of an amorphous WCoCN interlayer

Jia-Bin Yeh, Dung-Ching Perng, and Kuo-Chung Hsu

Institute of Microelectronics and Department of Electrical Engineering, National Cheng Kung University
No. 1 University Road, Tainan 701, Taiwan, Republic of China
E-mail: q1895137@mail.ncku.edu.tw, Tel: +886-6-275-7575 ext.62400-1260

1. Introduction

The integration of Cu wire with porous ultra low-k dielectric has been implemented to reduce RC delay for advanced Cu metallization [1]. Conventionally, PVD Ta/TaN bilayer structure was widely adopted as Cu diffusion barrier for IC industry [2-3]. However, the relatively thick sputtered additional Cu seed layer caused high wiring resistance, and poor Cu filling for sub-32 nm technology. Direct plate-able metal of Ru serve as a reliable seedless Cu barrier is a promising approach [4]. However, single Ru layer exhibited poor performance as Cu diffusion barrier due to its columnar grain structure [5,6]. Therefore, the research on improving direct plate-able Ru layer as seedless Cu barrier is urgent needed for advanced Cu metallization. Recently, bilayer barrier had been demonstrated its thermal stability against Cu penetration and also preserved its direct plate-able property [7-9]. In this study, we focused on thermal stability of Ru(5 nm)/WCoCN(5 nm) bilayer as a seedless Cu barrier system. The single 10 nm Ru layer as seedless copper barrier was baseline for comparison. The sheet resistance, GIXRD patterns, SEM top morphology, TEM images, and EDXS line scan were compared. The leakage currents of the Ru(5 nm)/WCoCN (5 nm) and single 10 nm Ru barrier layer on porous SiCOH were evaluated.

2. Experimental

A four inch p-type Si (100) wafer was cleaned using standard procedures. The stack of Cu/10 nm Ru/Si and Cu/5 nm Ru/5 nm WCoCN/Si were prepared by RF sputtering system. The working pressure was set to 8 mtorr with 8 sccm Ar gas flow rate. The WCoCN film was deposited using $W_{70}Co_3C_{27}$ target with gas mixture of 5 sccm Ar and 5 sccm N_2. Samples were performed rapid thermal annealing (RTA) in ULVAC MILA-5000 system at various temperatures for 30 min with vacuum level of 1×10^{-5} torr. Sheet resistances of the films were measured by four point probe. Phase identification were characterized by Rigaku D/MAX 2500 x-ray grazing incident angle diffraction (GIXRD) with CuKα radiation. Scanning electron microscopy (SEM) was employed to observe the morphology change of Cu surface. Energy dispersive X-ray spectroscopy (EDXS) line scan profiles were taken from the transmission electron microscopy (TEM) cross section for detecting the depth atomic concentration. The microstructure of the stacked Cu/diffusion barrier layers/p-SiOCH films was observed by TEM. Leakage current of the Cu/barrier/porous SiCOH/Si (MIS) structures were measured with Keithley-2361 instrument before and after the annealing process.

3. Results and Discussions

Sheet resistance measurement

Fig. 1 shows sheet resistance values of the Cu/5 nm Ru/5 nm WCoCN/Si and Cu/10 nm Ru/Si stacks after RTA annealing up to 700 ^oC for 30 min. For the single 10 nm Ru barrier, the sheet resistance drastically increased for annealing above 500 ^oC for 30 min possibly due to silicide formations. This illustrated the failure of the single 10 nm Ru barrier against Cu diffusion. In comparison, the sheet resistance of the 5 nm Ru/5 nm WCoCN bilayer barrier did not increase to very high level until 700^oC. Insertion of a 5 nm WCoCN interlayer between Ru and Si exhibited higher thermal stability and enhanced Cu barrier properties.

X-ray diffraction patterns

In Fig. 2, the two theta diffraction peaks at 43.31^o and 50.44^o corresponds to Cu(111) and Cu(200), respectively. In Fig. 2(a), the phases of Cu_3Si and Ru_2Si_3 formed after annealed at 500 ^oC for 30 min indicating the breakdown of the 10nm Ru barrier. In contrast, in Fig. 2(b), no Cu_3Si and Ru_2Si_3 peaks had been detected after annealing up to 600 ^oC for 30 min. With higher annealing temperature at 650 ^oC, Cu_3Si peaks appeared. In Fig. 3, phase transformation of the WCoCN/TEOS stack was characterized with elevated annealing temperatures. The diffraction spectra demonstrated that WCoCN film indeed had glassy structure and sustained amorphous phase at 600 ^oC for at least 30 min. These results reveal that the insertion of an amorphous 5 nm WCoCN interlayer clearly improves thermal stability by over 100 ^oC against Cu diffusion.

SEM observation

The morphology changes of Cu surface after high temperature annealing were evaluated by SEM. The Cu/Ru/Si stacks formed regular bright crystallites on top of the Cu surface after annealing above 500 ^oC (Fig. 4). The formation of Cu_3Si compound took place after annealing at 500 ^oC due to intermixing of Cu and Si. These results were consistent with XRD patterns and sheet resistance measurements.

Cross-sectional TEM/EDXS analysis

The cross-sectional TEM graphs and EDXS line scan depth profiles were employed to observe film's microstructure and copper's diffusion behavior. In Fig. 5(a), great amount of copper atoms diffused through 10 nm Ru was clearly observed after 600 ^oC annealing for 30 min. Small amount of copper exists in porous-SiOCH (p-SiOCH) layer could lead to high leakage current. This result clearly illustrates the failure of the 10 nm Ru barrier for preventing copper penetration. In contrast, in Fig. 5(b), copper atoms diffused through the first 5 nm Ru layer but the Cu signal drop rapidly right before the 5 nm WCoCN layer for the Cu/5 nm Ru/5 nm WCoCN/p-SiOCH sample. The results illustrate that Cu atoms accessibly penetrated through 5 nm Ru barrier rather than the 5 nm WCoCN layer. Nearly no copper atom signal was detected in p-SiOCH layer. The post 600 ^oC annealed Cu/Ru(5 nm)/WCoCN(5 nm) deposited on p-SiCOH had been examined by cross-sectional TEM (Fig. 6). The intact and sharp interface between 5 nm WCoCN and 5 nm Ru was clearly observed. The 5 nm WCoCN amorphous-like film can effectively block Cu diffusion.

Leakage current

Metal-insulator-silicon (MIS) structure using p-SiOCH as insulator was employed for leakage current testing. Fig. 7 is the J-E curves of the Cu /10 nm Ru/p-SiOCH/Si and Cu/5 nm Ru/5 nm WCoCN/p-SiOCH/Si MIS capacitors after annealing at 600 °C for 30 min. The 10 nm Ru barrier MIS sample exhibited a rapid rise in leakage current indicating massive Cu diffused into p-SiCOH. In contrast, the 5 nm Ru/5 nm WCoCN bi-layer barrier MIS structure provided three orders of magnitude in lower leakage currents, indicating that no considerable amount of Cu atoms diffused into p-SiOCH. This was attributed to the insertion of the 5 nm WCoCN layer which prevented the fast Cu diffusion into p-SiCOH during annealing.

4. Conclusion

In conclusion, we have demonstrated an improved Ru diffusion barrier by insertion of an amorphous WCoCN interlayer. The GIXRD pattern results of the bilayer barrier exhibited over 100 °C higher in thermal stability than that of single 10 nm Ru liner. The TEM graphs, EDXS depth profiles revealed that a 5 nm WCoCN layer was more effective blocking copper diffusion than a 5 nm Ru barrier. Ru barrier used for more advanced seedless Cu metallization can be realized with the insertion of 5 nm WCoCN layer. As a result, a robust Ru (5nm)/WCoCN (5nm) bilayer system could be a promising Cu barrier candidate in seedless Cu interconnects.

Acknowledgement

The authors would like to thank the Thin Film CRD group of United Microelectronic Co. for p-SiOCH film and TEM analysis. This work is supported by Taiwan's National Science Council under contract no. NSC 96-2221-E006-291 and by NCKU Landmark Project C004 grants.

References

[1]. Kajita, T., et al., Proceedings of IITC, 2003, p. 9.
[2]. M. H. Tsai, et al., J. Appl. Phys. 79 (1996) 6932.
[3]. G. S. Chen, et al., J. Vac. Sci. Technol. A 18 (2000) 720.
[4]. T. N. Arunagiri, et al., Appl. Phys. Lett. 86 (2005) 083104.
[5]. H. Kim, et al., J. Electrochem. Soc. 152 (2005) G594.
[6]. R. Chan, et al., Electrochem. Solid State Lett. 7 (2004) G154.
[7]. X. P. Qu, et al., Appl. Phys. Lett. 88 (2006) 151912.
[8]. L. C. Leu, et al., Appl. Phys. Lett. 92 (2008) 111917.
[9]. S. H. Kim, et al., J. Electrochem. Soc. 155 (2008) H589.

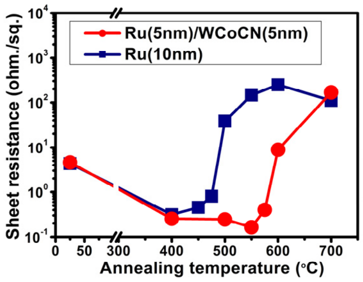

Fig. 1 Sheet resistances of the Cu/Ru(10nm)/Si and Cu/Ru(5 nm)/WCoCN(5 nm)/Si samples after annealing at various temperatures.

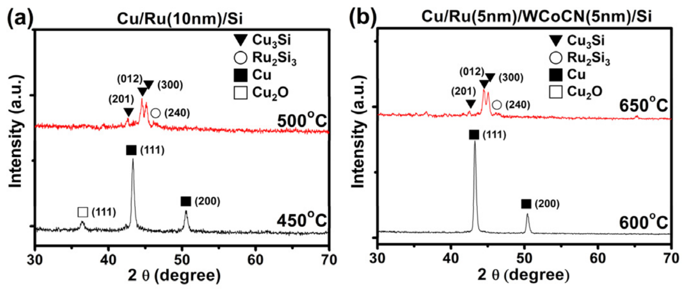

Fig. 2 X-ray diffraction patterns of the annealed (a) Cu/Ru (10 nm)/Si (b) Cu/Ru (5 nm)/WCoCN (5 nm)/Si.

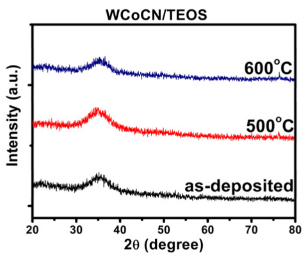

Fig. 3 X-ray diffraction patterns of the as-deposited and annealed WCoCN / TEOS stacked structures.

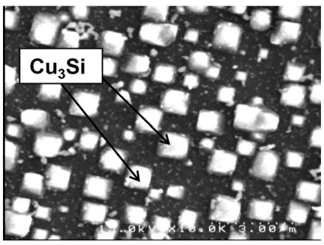

Fig. 4 SEM top views of the stacked Cu/10 nm Ru/Si structure after annealing at 500 °C for 30 min.

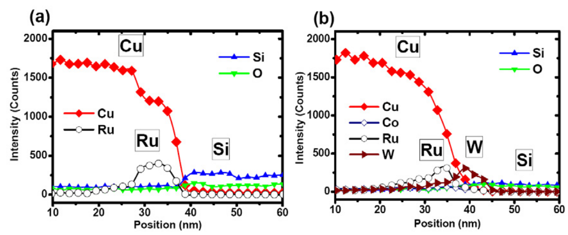

Fig. 5 The EDXS line scans taken from TEM graphs of (a) Cu/10 nm Ru/p-SiOCH (b) Cu/5 nm Ru/5 nm WCoCN/p-SiOCH after annealing at 600 °C for 30 min.

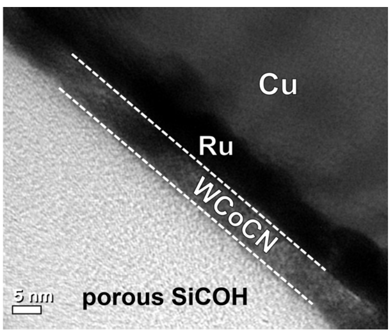

Fig. 6 Cross-sectional TEM image of the Cu / Ru / WCoCN / p-SiOCH structure after annealing at 600 °C for 30 min.

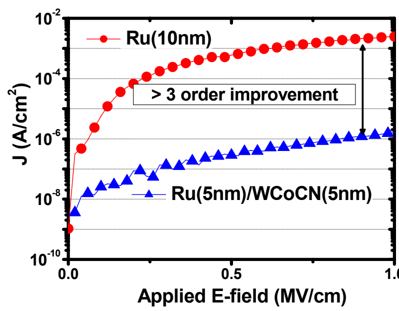

Fig. 7 MIS leakage current densities measured from the Cu/Ru and Cu/Ru/WCoCN deposited on p-SiOCH/Si after annealing at 600 °C for 30 min.